Supporting information for

Dopant-dependent Crystallization and Photothermal Effect of Sb-doped SnO_2 Nanoparticles as Stable Theranostic Nanoagents for Tumor Ablation

Nuo Yu,[a] Chen Peng,[b] Zhaojie Wang,[a] Zixiao Liu,[a] Bo Zhu,[a] Zhigao Yi,[c] Meifang Zhu,[a] Xiaogang Liu,[c] Zhigang Chen*, [a]

[a]State Key Laboratory for Modification of Chemical Fibers and Polymer Materials, College of Materials Science and Engineering, Donghua University, Shanghai 201620, China

[b]Department of Radiology, Shanghai Tenth People's Hospital, School of Medicine, Tongji university, Shanghai 200072, Peoples Republic of China

[c]Department of Chemistry, National University of Singapore, 3 Science Drive 3, Singapore 117543, Singapore

*Corresponding authors. E-mail: zgchen@dhu.edu.cn

1 Characterization and photothermal test

Morphology of samples were investigated by a high-resolution transmission electron microscopy (HR-TEM, JEM-2100F) equipped with energy dispersive spectroscopy (EDS). Powder X-Ray diffraction (XRD) patterns were recorded on a Bruker D4 X-ray diffractometer. The electronic states of elements were analyzed by using X-ray photoelectron spectroscopy (PHI-5400, Perkin-Elmer). The concentrations were determined using a Leeman Laboratories Prodigy high-dispersion inductively coupled plasma atomic emission spectroscopy (ICP-AES, Prodigy) by dissolving the samples into regia solution followed by the heat treatment at 120 °C for 12 h. The Fourier transform infrared (FTIR) spectrum was acquired from samples in KBr pellets using an IRPrestige-21 spectrometer (Shimadzu). UV-vis-NIR absorption spectra were measured by UV–vis–NIR spectrophotometer (Shimadzu UV-3600). Hydrodynamic size

distribution was carried out with the Zatasizer (Malvern). Hydrodynamic size distribution was carried out with the Zatasizer Nano Z (Malvern).

To measure the photothermal properties of the samples, 1064-nm semiconductor laser (SFOLT Co. Ltd, Shanghai, China) was used to irradiate a plastic tube containing water or undoped/doped SnO_2 aqueous dispersion (0.1 mL). The infrared thermal images and temperature were recorded using an infrared camera (A300; FLIR systems Inc.).

2 Calculation of photothermal conversion efficiency

The photothermal transduction efficiency was calculated using below equations as:

$$\eta_T = \frac{hA(\Delta T_{max,dis} - \Delta T_{max,H2O})}{I(1 - 10^{-A_{1064}})} \quad \text{(S1)}$$

where h, A, I, and A_{1064} respectively denote the heat transfer coefficient, the surface area of the container, the laser power (250 mW), and the absorbance (0.6006) of the dispersion at 1064 nm. $\Delta T_{max,dis}$ and $\Delta T_{max,H2O}$ are the temperature change of the nanocrystal dispersion and deionized water at the equilibrium maximum temperature (**Fig. 5b**). The value of hA can be calculated from equation (S2) as：

$$\tau_s = \frac{m_{H2O} C_{H2O}}{hA} \quad \text{(S2)}$$

where the system time constant τ_s is respectively determined to be 113 and 112 s for $Sb_{0.2}$-SnO_2 and deionized water in **Fig. 5c,d** (Here we defined the τ_s as 113); m_{H2O} and C_{H2O} are the mass (0.1 g) the heat capacity (4.2 J g^{-1}) of deionized water. Therefore, we can calculate the η_T of the present nanocrystals to be 48.3 %.

3 Figures

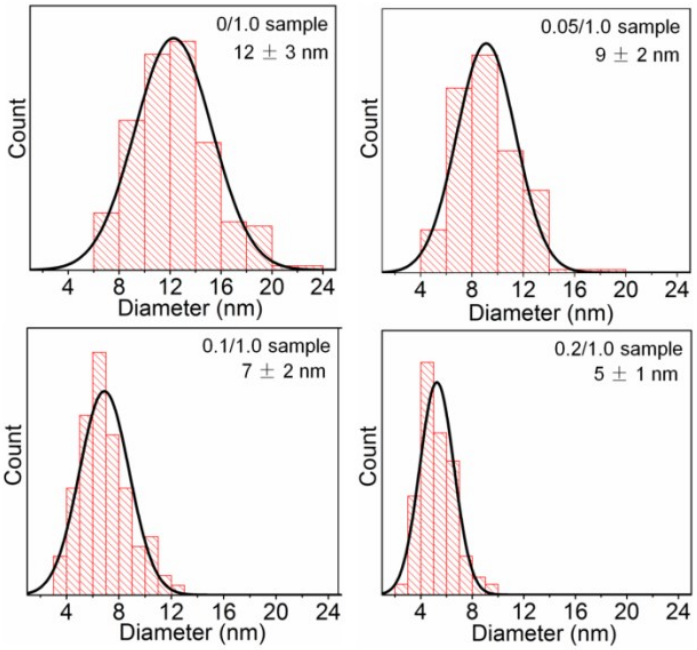

Fig. S1 Size distributions of the pure and Sb-doped SnO_2 samples.

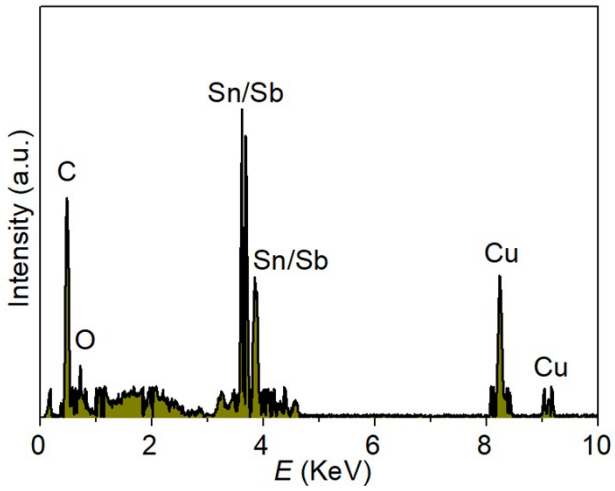

Fig. S2 EDS pattern of $Sb_{0.2}$-SnO_2 nanocrystals.

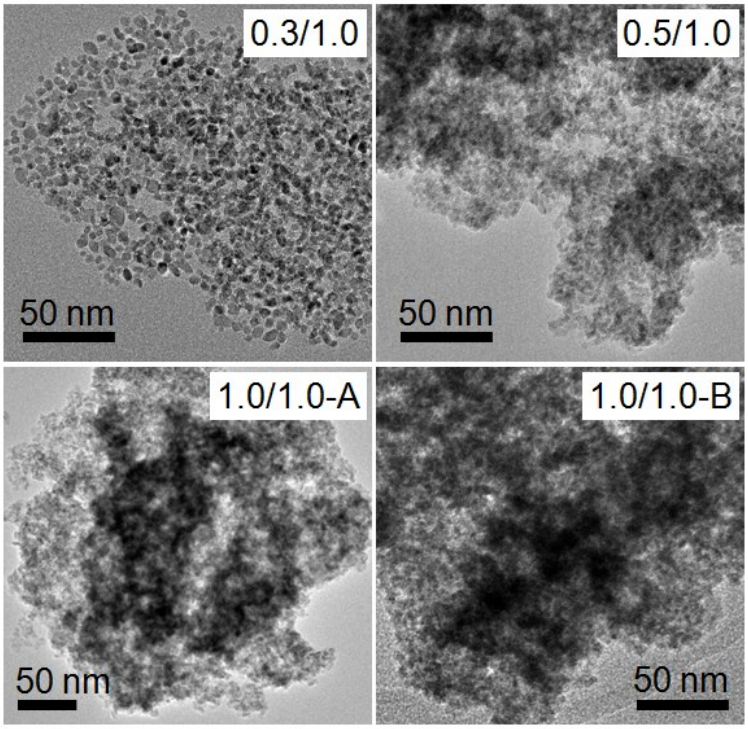

Fig. S3 TEM images of 0.3/1.0, 0.5/1.0, 1.0/1.0-A and 1.0/1.0-B samples.

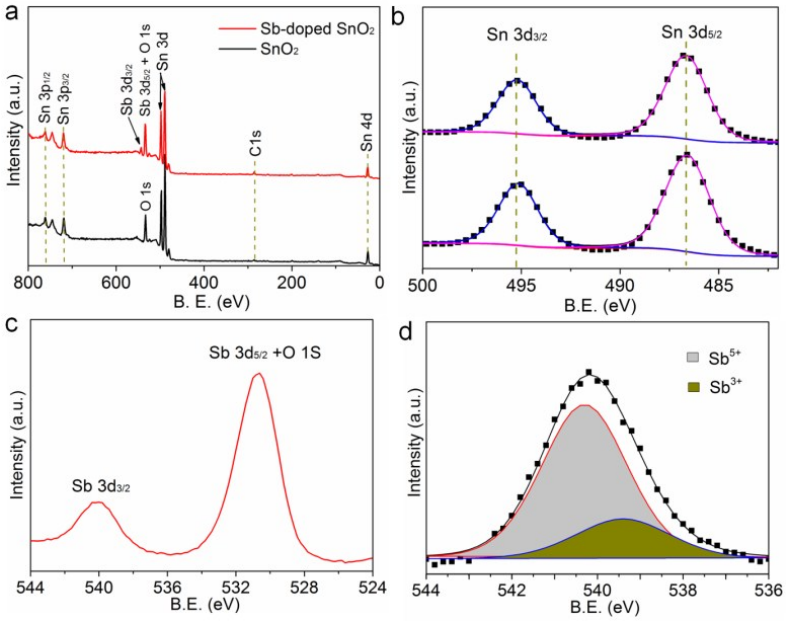

Fig. S4 (a) Survey XPS spectra and (b) Sn 3d spectra of the undoped SnO_2 sample and $SbCl_3/SnCl_4$= 0.2/1.0 sample. (c) Sb 3d spectrum of $SbCl_3/SnCl_4$ = 0.2/1.0 sample. (d) The deconvolution of Sb $3d_{3/2}$ peak.

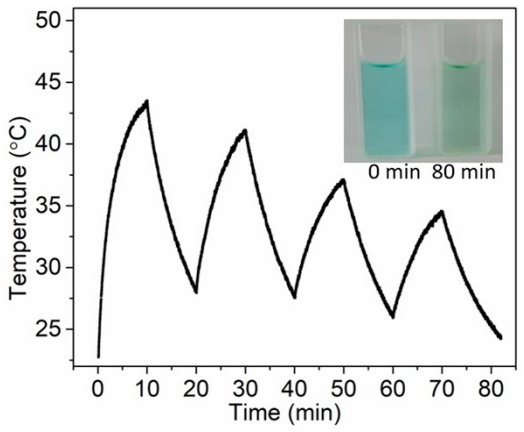

Fig. S5 Temperature curve of ICG solution during laser ON/OFF cycles (808 nm, 2.0 W cm^{-2}). The inset shows the color change of ICG solution before and after irradiation.

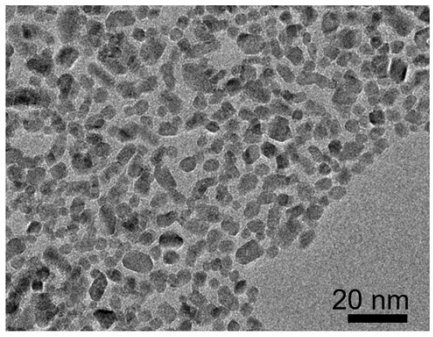

Fig. S6 TEM image of $Sb_{0.2}$-SnO_2 nanocrystals after laser irradiation.

Fig. S7 Photograph of $Sb_{0.2}$-SnO_2 nanocrystals dispersed in chloroform with the addition of one drop of oleic acid.

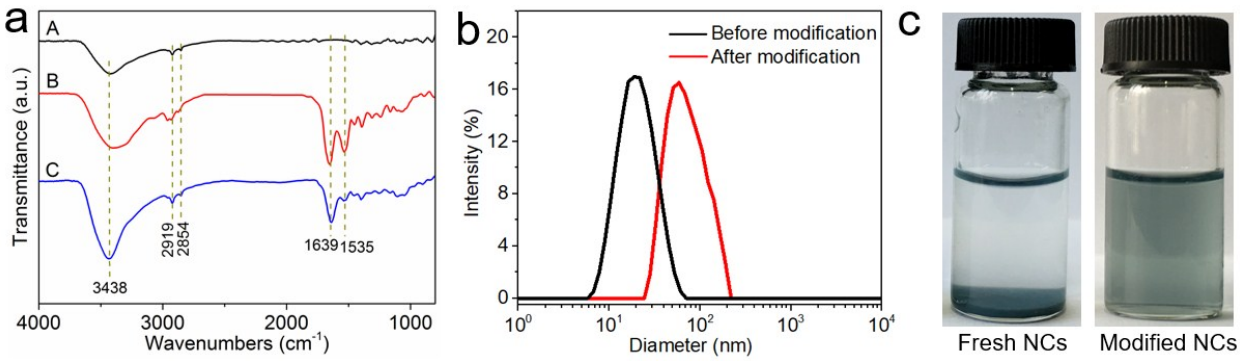

Fig. S8 (a) FT-IR spectra of A: fresh NCs, B: BSA, and C: BSA-modified NCs. (b) Hydrodynamic sizes of $Sb_{0.2}$-SnO_2 nanocrystals before and after BSA modification. c) Photograph of fresh nanocrystals and BSA-modified nanocrystals dispersed in PBS, respectively.

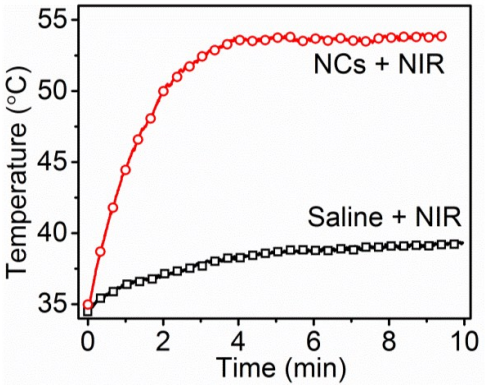

Fig. S9 Temperature elevation curves of mice at post-injection of nanocrystals or saline under the irradiation of 1064-nm laser with the intensity of 1.0 W cm^{-2}.